



Investigation on performance of zirconia and magnesia–zirconia stationary phases in hydrophilic interaction chromatography

Qing Wang^a, Jing Li^a, Xin Yang^a, Li Xu^a, Zhi-guo Shi^{b,*}, Lan-Ying Xu^c

^a Tongji School of Pharmacy, Huazhong University of Science and Technology, Wuhan 430030, China

^b Department of Chemistry, Wuhan University, Wuhan 430072, China

^c Hubei Key Laboratory of Economic Forest Germplasm Improvement and Resources, Comprehensive Utilization, Huanggang Normal University, Huangzhou, China

ARTICLE INFO

Article history:

Received 10 March 2014

Received in revised form

5 June 2014

Accepted 10 June 2014

Available online 19 June 2014

Keywords:

Zirconia

Magnesia–zirconia

Hydrophilic interaction chromatography

ABSTRACT

In the current study, zirconia (ZrO_2) and its composite, magnesia–zirconia ($MgO-ZrO_2$), were prepared as the hydrophilic interaction chromatographic (HILIC) stationary phases (SPs). Different experimental variables including water content, pH and buffer concentration in the mobile phase (MP) as well as column temperature were systematically studied to permit an in-depth understanding of the chromatographic properties of the mentioned SPs and to explore the retention mechanism further on. The results were compared with a native SiO_2 column. Adsorption was demonstrated as the main retention mechanism on the two ZrO_2 -based SPs. The transferring of the analytes from the MP to the ZrO_2 -based SPs was endothermic and high column temperature would facilitate the retention. In addition, the $MgO-ZrO_2$ SP exhibited superior resolution, column efficiency as well as stronger retention in comparison to the bare ZrO_2 SP, which demonstrated that the introduction of MgO could improve the structure and properties of the material. In conclusion, $MgO-ZrO_2$ was a promising material for HILIC applications.

© 2014 Elsevier B.V. All rights reserved.

1. Introduction

Zirconium dioxide (zirconia, ZrO_2), thanks to its remarkable thermal stability (can withstand high temperature up to 200 °C in chromatographic separation [1–3]), pH stability in the range of 1–14, mechanical stability as well as its particular surface chemical properties, has become one of the alternative metallic oxide-based chromatographic stationary phases (SPs) to silica (SiO_2) [4,5]. The surface of ZrO_2 is far more intricate than that of native SiO_2 , containing a number of distinct classes of interaction sites including Brønsted acid, Brønsted base and Lewis acid sites [6]. Zirconium ion (IV) is a strong Lewis acid that exhibits electropositivity and has an affinity for Lewis bases that donate lone pair electrons to form coordination compounds, which is called ligand-exchange interaction. Besides, ZrO_2 is an amphoteric metallic oxide, the hydroxyl groups of which can be protonated or deprotonated depending on the environmental pH, acting as either anion- or cation-exchanger respectively [7]. Owing to these special surface chemistry properties, ZrO_2 -based SPs exhibit distinct chromatographic properties compared to common chromatographic SPs like SiO_2 -based SPs. However, native ZrO_2 generally exhibits low

column efficiency due to the poor pore structure ('ink-bottle' shaped pores) and the chemically heterogeneous surface [8,9].

To improve the chromatographic performance of ZrO_2 -based SPs, hybrid ZrO_2 oxides, such as titania (TiO_2)– ZrO_2 [10], SiO_2 – ZrO_2 [11], ceria– ZrO_2 [12,13] and magnesia (MgO)– ZrO_2 [8,11,14], were developed. For example, $MgO-ZrO_2$ was demonstrated to possess enhanced specific surface area, improved specific pore volume and pore connectivity [8,14], resulting in higher column efficiency than the bare ZrO_2 SP [8,11].

Hydrophilic interaction chromatography (HILIC) was first named by Alpert [15], which was based on a polar SP and a relatively nonpolar binary eluent in which 3–40% [16] water acted as the stronger eluting component, and acetonitrile (ACN, a water-miscible organic eluting component) as the weaker one. Although there was still dispute about the retention mechanism in HILIC [17–19], an agreement that the retention mechanism was largely dependent on the SP, MP and the analytes was generally reached. HILIC has emerged as a complementary chromatographic mode to reversed-phase liquid chromatography (RPLC) especially for the separation of polar and hydrophilic analytes. However, the commercial HILIC SPs were almost based on silica or polymer matrices, and selection of HILIC SPs for application was random for lack of theory guidance. Therefore, it is important to prepare new SPs as alternatives to silica or polymer matrices, expand their applications, as well as investigate the retention mechanism in HILIC.

* Corresponding author. Tel.: +86 27 68752701; fax: +86 27 68754067.
E-mail address: shizg@whu.edu.cn (Z.-g. Shi).

As hydroxyl groups and zirconium ions (IV) exist on the surface, ZrO_2 is highly supposed to be an appropriate SP for HILIC. However, few reports were found about its application for HILIC. Kučera and co-workers [20,21] compared the HILIC retention behavior of a set of hydrophilic analytes on polybutadiene modified ZrO_2 , carbon-coated ZrO_2 , bare ZrO_2 and SiO_2 -based columns. In their study, adsorption and ligand-exchange interactions were found to be the primary retention mechanism on ZrO_2 -based columns, while partitioning was on the SiO_2 -based column. In addition, Randon et al. prepared a SiO_2 - ZrO_2 composite monolithic SP by generating ZrO_2 coating on the SiO_2 monolithic column [4]. The investigation of the retention mechanism revealed that partitioning was not the unique retention interaction on the SiO_2 - ZrO_2 monolithic column. Separation of three dimethylxanthine isomers which was difficult to be realized with RPCLC was accomplished on the SiO_2 - ZrO_2 column in HILIC mode.

Considering the lack of systematic study on the retention mechanism of ZrO_2 SPs in HILIC, and there was no report on the application of hybrid ZrO_2 materials for HILIC, in this study, ZrO_2 and MgO - ZrO_2 were employed as HILIC SPs. Effects of several chromatographic parameters on retention of a set of test solutes were studied in detail to explore the retention mechanism of the two ZrO_2 -based SPs.

2. Experimental

2.1. Chemicals

Sulfamerazine, sulfamethazine, sulfathiazole, sulfadiazine, propranolol and procaine were obtained from Alfa Aesar (Tianjin, China). Isoniazide, adenine, phenytoin, berberine, thymine and quinine were purchased from Aladdin (Shanghai, China). Tetracaine and clonidine were bought from Tokyo Chemical Industry Co. Ltd. (Tokyo, Japan). ACN (HPLC grade), methanol (HPLC grade), acetic acid (HAc), ammonia, ammonium acetate (NH_4Ac), zirconium(IV) oxychloride octahydrate ($ZrOCl_2 \cdot 8H_2O$), magnesium chloride hexahydrate ($MgCl_2 \cdot 6H_2O$), ethanol, petroleum ether (60–90 °C) and isopropanol were purchased from Sinopharm Chemical Reagent Co., Ltd. (Shanghai, China). Polyoxyethylene sorbitan trioleate (Tween 85) and sorbitan monooleate (Span 80) were obtained from Shanghai General Chemical Reagent Factory (Shanghai, China). Ultrapure water was produced by a Heal Fore NW system (Shanghai, China).

2.2. Instrumentation

HPLC analysis was performed on a Dionex Ultimate 3000 chromatographic system (California, USA) which consisted of a degasser, two Ultimate 3000 pumps, an Ultimate 3000 automated injector, an Ultimate 3000 RS column compartment and a diode array detector. For data acquisition and analysis, the Chromeleon software was used. The Zeta potential was measured by a ZetaPALS high resolution Zeta potential analyzer (Brookhaven, USA).

2.3. Preparation of MgO - ZrO_2 and ZrO_2 columns

MgO - ZrO_2 microparticles were synthesized according to the procedures elaborated in the previous work [8,11]. Briefly, $ZrOCl_2 \cdot 8H_2O$ and $MgCl_2 \cdot 6H_2O$ were dissolved in pure water, and the mixture was then put into petroleum ether which contained Span 80 and Tween 85. The mixture was sheared and emulsified by a shear emulsifying mixer to form the emulsion. Ammonia gas was generated by heating ammonia aqueous solution and channeled into the emulsion for 2 h. White precipitation was obtained and separated by filtration, followed by washing with copious ethanol, petroleum ether and water. The microparticles were dried and sintered to burn off organic residues. Size classification was performed in a precipitation/decanting/resuspension order. Particles of 5 μm in diameter were collected, homogenized with isopropanol afterwards, and then pumped into the

stainless steel columns (150 mm \times 2.1 mm i.d., IDEX Health & Science LLC, MA, USA). ZrO_2 microparticles were synthesized as the same procedure of MgO - ZrO_2 without adding $MgCl_2 \cdot 6H_2O$. Scanning electron microscope (SEM) was carried out using a JSM-35CF instrument (JEOL, Tokyo, Japan). Fourier transform infrared spectroscopy (FT-IR) was performed on AVATAR 360 (Thermo, USA).

The bare SiO_2 column (150 mm \times 2.1 mm i.d., 5 μm) used for comparison was from Kromasil (Akzo-Nobel, Amsterdam, Netherlands).

2.4. Chromatographic evaluation

Stock solutions (1 mg/mL) of test solutes were prepared by dissolving the appropriate amount of each compound separately in methanol. These solutions were further diluted to get the working solutions (10 $\mu g/mL$) with the MP, prior to injection.

The following chromatographic conditions remained constant throughout the study: a flow rate of 0.2 mL/min, an injection volume of 5 μL . The column temperature was 25 °C except specified.

When NH_4Ac buffers were applied, the NH_4Ac concentration referred to the amount of NH_4Ac in the aqueous phase of the MP. Prescribed amount of NH_4Ac was dissolved in water to form the NH_4Ac solution and the required pH of it was adjusted by HAc or ammonia. And the pH value of the MP referred to the pH of aqueous phase, which was adjusted prior to mixing with ACN.

The void volume was calculated by dead time which was measured by injection of pure ACN. The retention time of the solutes was determined at least in triplicates all through the experiments. The measurement of retention was expressed as retention factor (k') for all the analytes.

2.5. Stability test

The stability test was performed with the MP of 97% ACN-3% of 50 mM NH_4Ac buffer at a pH of 6.0. k' and the theoretical plates of two probe analytes, i.e. sulfathiazole and sulfadiazine, were monitored to evaluate the stability of the two ZrO_2 -based columns.

3. Results and discussion

3.1. Characterization of synthesized MgO - ZrO_2 and ZrO_2 microparticles

SEM images of MgO - ZrO_2 and ZrO_2 microparticles are shown in Fig. 1. Both the two microparticles are spherical and in the size of $\sim 5 \mu m$. FT-IR spectra of ZrO_2 and MgO - ZrO_2 are depicted in Fig. 2. The absorption peak at around 3427 cm^{-1} should be ascribed to the vibration of $-OH$ on the surface of MgO - ZrO_2 and ZrO_2 . In the spectrum of ZrO_2 , the absorption peaks appeared at 450.2, 514.2, 578.1 and 729.0 cm^{-1} corresponded to the stretching vibration of $Zr-O$. However, the strong characteristic peak of $Mg-O$ at 500.1 cm^{-1} occurred in the spectrum of MgO - ZrO_2 , which masked the characteristic peaks of $Zr-O$. Based on the above analysis, ZrO_2 and MgO - ZrO_2 were successfully prepared.

3.2. Selectivity of the two ZrO_2 -based columns

In the preliminary experiment, a wide range of analytes containing acids (salicylic acid and its derivatives, benzoic acid, nicotinic acid and cyanuric acid), bases (sulfonamides, alkaloids, local anesthetics and nucleic acid bases) and neutrals (benzene, phenanthrene, naphthalene and biphenyl) were employed to investigate the selectivity of MgO - ZrO_2 and ZrO_2 SPs in HILIC mode. The acidic compounds showed asymmetric and deformed peaks on the ZrO_2 column; however, there was no signal on the

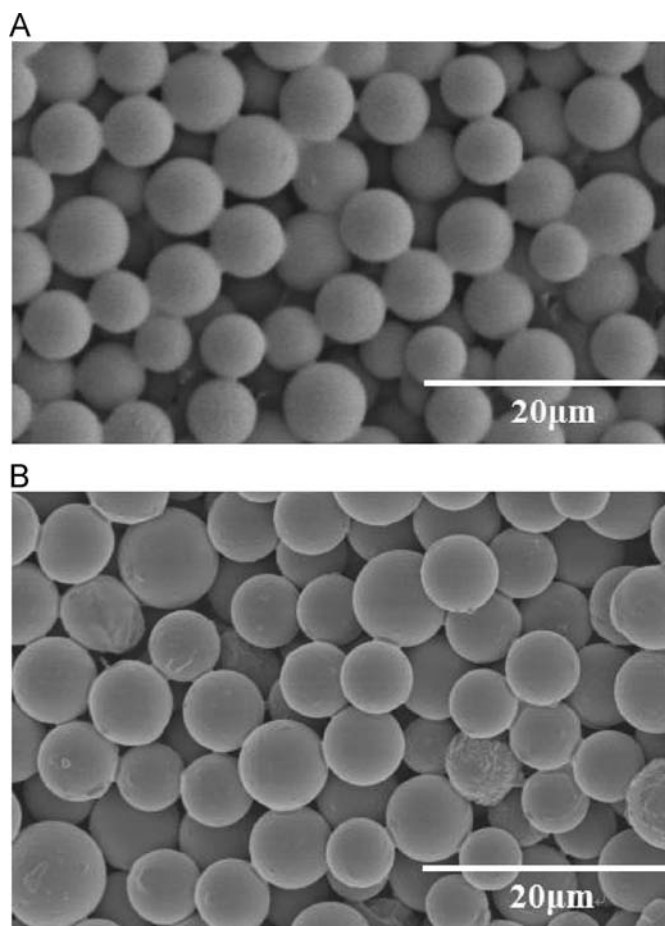


Fig. 1. SEM images of (a) ZrO_2 and (b) $MgO-ZrO_2$.

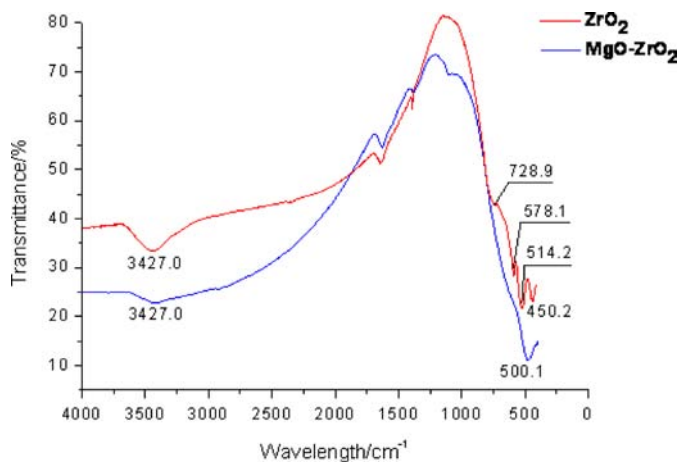


Fig. 2. FT-IR spectra of ZrO_2 and $MgO-ZrO_2$.

$MgO-ZrO_2$ column. The most possible reason for this observation was that, owing to the introduction of MgO , the surface of $MgO-ZrO_2$ microparticles became more alkaline compared to the bare ZrO_2 material [8]. As a result, the adsorption interaction between acidic analytes and the $MgO-ZrO_2$ was strengthened [11]. For neutrals, no retention was observed when altering the MP conditions on the two ZrO_2 -based columns. As for the basic analytes, peaks were symmetrical and the retention was reasonable. Therefore, a series of basic analytes were selected as the test solutes for the subsequent studies.

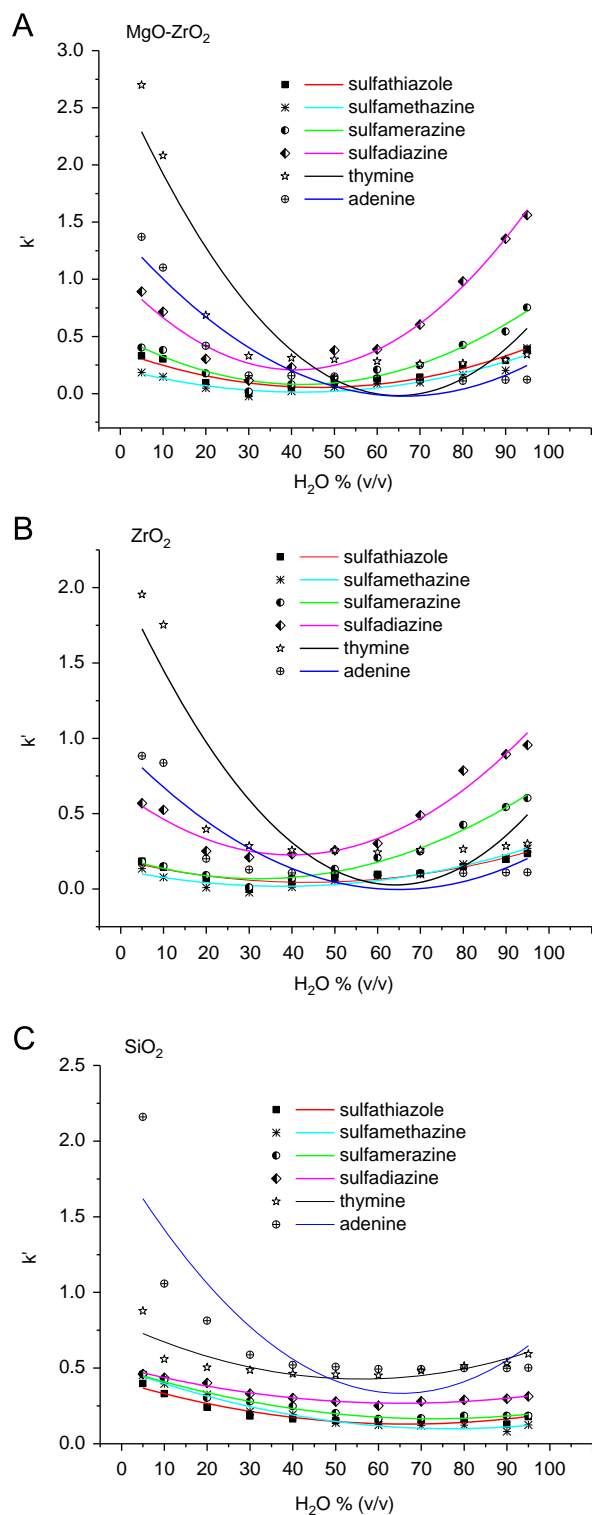


Fig. 3. Influence of water content on k' of the test solutes. (A) $MgO-ZrO_2$; (B) ZrO_2 ; (C) SiO_2 . MP: different ratios of ACN and pure water. Column temperature: 25 °C.

3.3. Investigation of the effect of different chromatographic parameters on retention

3.3.1. Effect of water content in the MP

Fig. 3 shows the influence of water content in the MP on the k' of target analytes by varying ratios of ACN and pure water in the MP. Retention behavior was similar to each other on the two ZrO_2 -based columns. A “U-shape” curve was generally obtained correlating the

water content in the MP with the k' . Specifically, k' dropped with the increasing ACN content in the water-rich region while the opposite trend could be seen in the ACN-rich region, which signified that the retention mechanism was the combination of HILIC and RPLC [20].

On MgO–ZrO₂ and ZrO₂ columns, for adenine and thymine, only negligible retention was observed in the water-rich region, whereas k' apparently raised when the water content decreased from 60% down to 5%. On the contrary, for sulfonamides, the retention was stronger in the water-rich region than that in ACN-rich region. This might be ascribed to the different Log $P_{o/w}$ values (see Table 1) of the nucleic acid bases and sulfonamides. Adenine and thymine were more hydrophilic compared to sulfonamides, and they thus presented more obvious hydrophilic property with bigger k' values in the ACN-rich region. However, RPLC mechanism became prominent in the water-rich region. Therefore, the relatively hydrophobic sulfonamides exhibited stronger retention.

Compared to the two ZrO₂-based columns, as shown in Fig. 3(C), all the studied compounds exhibited weaker retention except adenine on the native SiO₂ column. The retention only slightly strengthened as the water content increased from 60% to 95%; while in the ACN-rich region, typical HILIC behavior was observed. In addition, the crossed curves in Fig. 3 revealed that the elution order of the studied analytes changed with the water content in the MP on the three columns.

The retention in HILIC mode was primarily a multimodal process as mentioned above. To gain a deep insight on the retention mechanism in the HILIC region (this region was analyte-dependent as the break points of the “U-shape” curves varied among the analytes) on the three columns, experimental data in this region were collected and analyzed according to the two well-established empirical models as below. Eq. (1) describes partitioning mechanism [17,22–24] when taking into account of elution strength of water and ACN in HILIC:

$$\log k = \log k_{\text{ACN}} - S \Phi_w \quad (1)$$

where k and k_{ACN} represent, respectively, the retention factor in the water–ACN MP and in pure ACN (the weakest solvent herein). Φ_w is the volume fraction of the strongest eluent (water herein), and S is the obtained slope derived from a plot of $\log k$ versus Φ_w . However, a linear plot of $\log k$ versus $\log N_{\text{water}}$ (logarithm of mole fraction of water in the MP) should be an indication of adsorption mechanism [17,22–24]:

$$\log k = \log k_{\text{water}} - \frac{As}{n_{\text{water}}} \log N_{\text{water}} \quad (2)$$

where k_{water} is the retention factor in pure water phase (the strongest solvent here). As and n_{water} are the cross-sectional areas occupied by the solute and water molecules on the surface, respectively.

According to the two equations above, $\log k$ was plotted against Φ_w (1) and $\log N_{\text{water}}$ (2), respectively. The linear correlation coefficients (r^2) of the studied analytes on the three columns are listed in Table 2. As shown in this table, 0.7149–0.9315 and 0.7152–0.9485 for r_1^2 between $\log k$ and Φ_w were obtained on MgO–ZrO₂ and ZrO₂ columns, respectively; while, dependency of $\log k$ on $\log N_{\text{water}}$ fitted better with the linear regression curve, and r_2^2 values were in the range of 0.9207–0.9995 and 0.9684–0.9999, respectively. Obviously, the coefficients obtained were closer to 1 for the adsorption model instead of the partitioning one, which signified that retention on the two ZrO₂-based columns was more probably based on adsorption interaction. This conclusion was consistent with previous studies focusing on the retention mechanism on bare ZrO₂ column in HILIC [21,22]. Moreover, from the chemical surface properties, the two ZrO₂-based columns had the capacity to interact with the analytes through hydrogen bonding, electrostatic, dipole–dipole, ligand-exchange interactions, etc., all of

which could contribute to adsorption interaction. However, for the SiO₂ column, r_2^2 was not always larger than r_1^2 , which revealed that adsorption and partitioning interaction participated simultaneously in retaining the analytes.

3.3.2. Effect of buffer concentration

The buffered MP would improve the peak shape, separation efficiency and selectivity, inhibit electrostatic interaction as well as ensure consistent results over time. Among different buffer salts, NH₄Ac was commonly used in HILIC owing to its good solubility in organic solvents and compatibility with the subsequent detector, such as mass spectrometry. In the present study, effect of NH₄Ac concentration on retention was evaluated in the range of 5–110 mM for the three columns.

Fig. 4 depicts the influence of the concentration of NH₄Ac on retention behavior of the model compounds at a constant pH of 6.0. The data of propranolol and melamine were absent at the concentration of 5 mM NH₄Ac in Fig. 4(A) and (B) as they were not eluted from the two ZrO₂-based columns. And data of sulfonamides were unavailable for the bare SiO₂ column in this section and also on the following investigation of pH and column temperature parts as they co-eluted with the solvent.

It was evident that k' of the analytes decreased with the increasing NH₄Ac concentration on the three SPs. This can be explained that most of the target analytes existed in their protonated form, while the SP may be ionized at the investigated pH of 6.0 based on the Zeta potential values in Table 3. Therefore, ion exchange, hydrogen bonding and electrostatic attraction interactions may contribute to the retention. However, these interactions would be weakened with the increasing NH₄Ac concentration. For example, the electrostatic attraction interaction would be shielded [18] because the increasing NH₄Ac would gather around the charged groups [24,25] resulting from both the ionized analytes and SP surface, leading to the decreased retention. In addition to the above-mentioned interactions, for the two ZrO₂-based columns, ligand exchange was involved; however, it may be suppressed as access of the analytes to the zirconium ions (IV) might be significantly hindered by the surrounding NH₄Ac. Another probable explanation was that acetate ions were Lewis base, and played a competitive role to the analytes for Lewis acid sites on the ZrO₂-based SPs [23], which led to the weakened retention. Furthermore, as a kind of Kosmotrope salt [26], acetate ions mainly existed in the water-rich layer on the surface of the SP and they would interact strongly with the water molecules, leading to weakened interaction between the analytes and the immobilized water molecules on the SP. As a result of the individual or combinational above factors, the increasing concentration of NH₄Ac led to the gradual weakened retention of the analytes.

3.3.3. Effect of MP pH on retention

The pH of MP has a great influence on the ionization of the target compounds as well as the SP surface, and thus alters the retention performance, especially when the SP matrix exhibits diverse properties across the studied pH range. For example, ZrO₂ is amphoteric, which could be protonated or deprotonated resulting in positively or negatively charged surface under different pH conditions. Hence, this parameter deserved careful evaluation for the two ZrO₂-based columns.

Effect of MP pH on retention was investigated from pH 4.0 to 13.0 for the two ZrO₂-based columns as MgO would be dissolved at the pH ≤ 3.0. However, it is well known that the native SiO₂ can endure the MP pH < 8.0 [3,11], and hence pH of within the range of 3.0–7.5 was studied on SiO₂ column. Fig. 5 depicts the k' changes of target solutes with the MP pH. For the most analytes,

Table 1
The properties of test analytes used in this study.

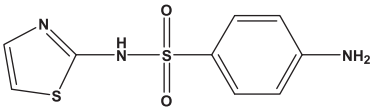
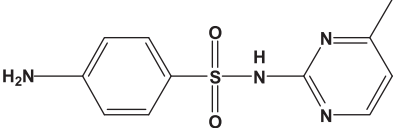
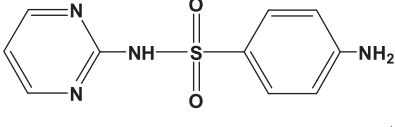
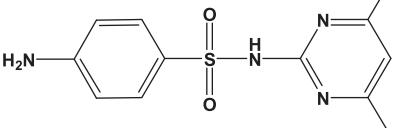
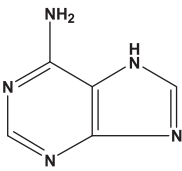
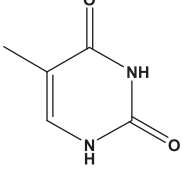
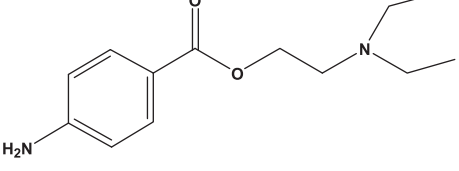
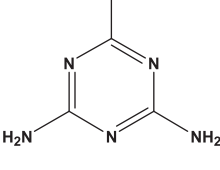
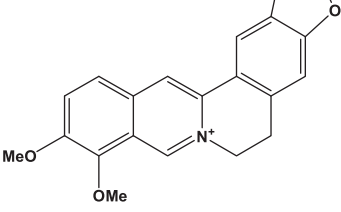
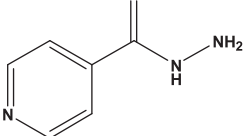
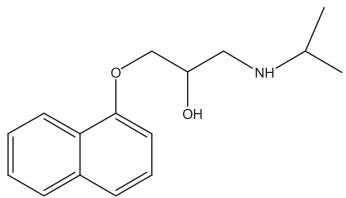
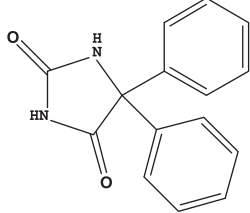
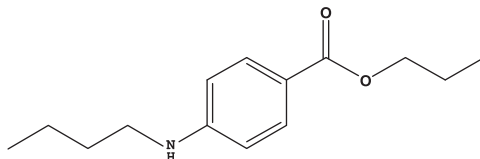
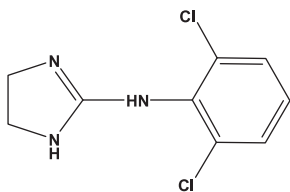
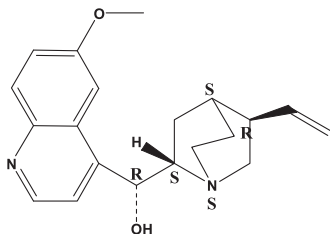
Analyte	Structure	Molecular weight	pKa	Log Po/w
Sulfathiazole		255	7.24 ± 0.1	0.005 ± 0.310
Sulfamerazine		264	7.35 ± 0.1	0.107 ± 0.267
Sulfadiazine		250	6.81 ± 0.1	-0.074 ± 0.255
Sulfamethazine		278	7.89 ± 0.1	0.296 ± 0.278
Adenine		135	9.42 ± 0.2	-2.133 ± 0.465
Thymine		126	9.24 ± 0.1	-0.621 ± 0.214
Procaine		236	9.24 ± 0.25	2.256 ± 0.523
Melamine		126	5.39 ± 0.10	-1.370 ± 0.187
Berberine		336	-	-
Isoniazide		137	11.40 ± 0.10	-0.766 ± 0.245

Table 1 (continued)

Analyte	Structure	Molecular weight	pKa	Log Po/w
Propranolol		295	9.50 ± 0.30	2.900 ± 0.247
Phenytoin		252	8.28 ± 0.10	1.421 ± 0.369
Tetracaine		264	8.24 ± 0.28	3.749 ± 0.541
Clonidine		230	8.10 ± 0.50	2.362 ± 0.603
Quinine		324	9.28 ± 0.70	2.823 ± 0.431

Data were obtained from SciFinder.

Table 2

Linear correlation coefficients of studied analytes in two retention models i.e. partitioning and adsorption.

Analyte	MgO–ZrO ₂		ZrO ₂		SiO ₂	
	r ₁ ²	r ₂ ²	r ₁ ²	r ₂ ²	r ₁ ²	r ₂ ²
Sulfathiazole	0.7470	0.9569	0.7152	0.9995	0.6988	0.9393
Sulfamethazine	0.8125	0.9833	0.7685	0.9865	0.9903	0.9339
Sulfamerazine	0.7629	0.9379	0.9258	0.9843	0.9029	0.9789
Sulfadiazine	0.7149	0.9207	0.8551	0.9999	0.9946	0.9237
Adenine	0.9315	0.9995	0.8524	0.9684	0.8979	0.9354
Thymine	0.8166	0.9606	0.9485	0.9938	0.8796	0.9991

r₁² refers to the correlation coefficient of the plot of logk versus ϕ_w ; r₂² refers to the correlation coefficient of the plot of logk versus log N_{water}.

k' on the two ZrO₂-based columns increased slightly with the increasing pH from 4.0 to 8.0; while, over half of them could not be eluted when the pH value reached 11.5 or above (data at these pH values were not shown). This might be due to the amphoteric surface of ZrO₂. At low pHs, since the interaction sites of the SP exhibited as anion exchangers, and the majority of the analytes

were weak bases which were prone to be protonated, electrostatic repulsion may exist between the SP and analytes, resulting in the relatively weak retention. However, the interaction sites on the SP acted as cation exchangers at high pH values, and with the raised pH, protonation of the analytes was weakened but a complete deprotonation could not be reached (pKa > 8.0 for most test solutes in Table 1). Therefore, ion-exchange interaction replaced electrostatic repulsion gradually, leading to the increasing retention. As a comparison, k' of the analytes on the native SiO₂ column gradually increased. Under the studied pH range from 3.0 to 7.5, the analytes were protonated while the surface of SiO₂ was negatively charged and exhibited cation-exchange interaction which became stronger with the elevated MP pH.

3.3.4. Effect of column temperature

Column temperature is an important factor in HILIC separations [27–29] as it influences significantly on the following properties: (i) diffusivity of the analytes; (ii) viscosity of the MP, which is closely correlated with hydrophobicity and hydrophilicity of the MP; (iii) enthalpy and entropy change of the analytes in the transferring process from the MP to SP; (iv) pKa of the analytes

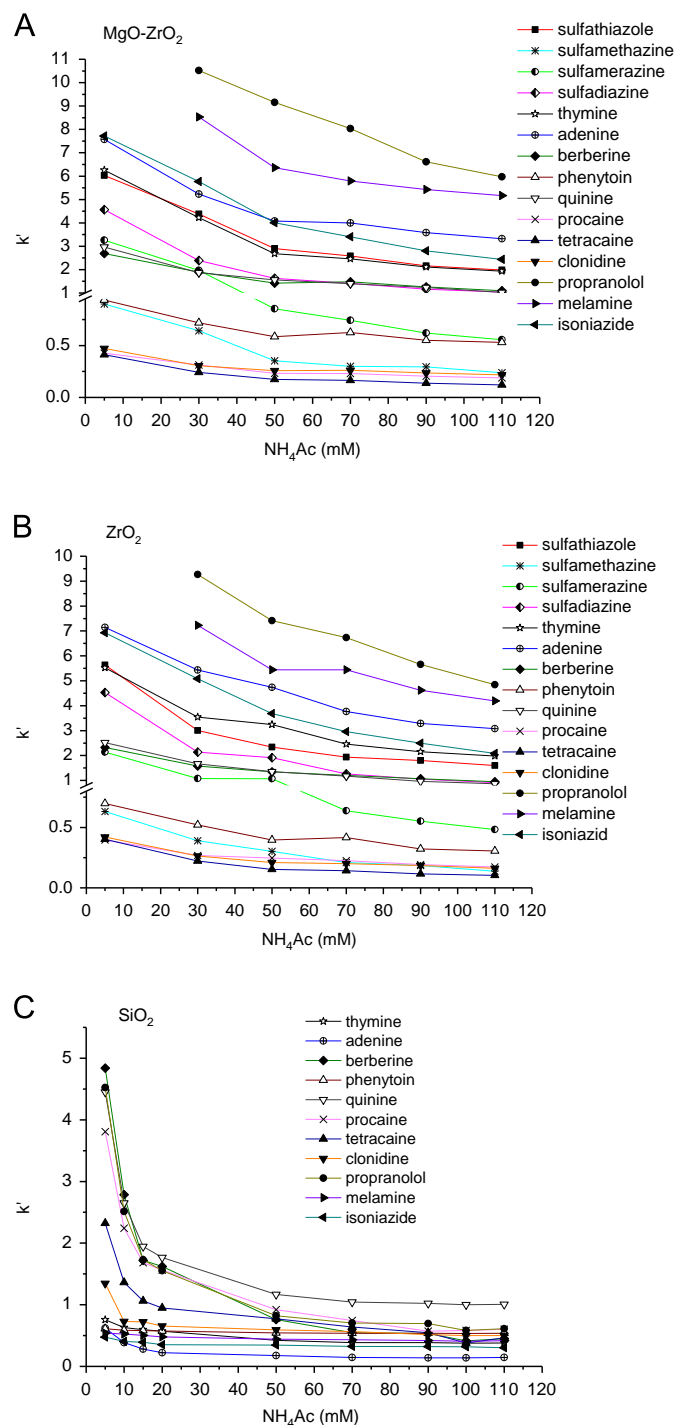


Fig. 4. Influence of NH_4Ac concentration on k' of the test solutes. (A) MgO-ZrO_2 ; (B) ZrO_2 ; (C) SiO_2 . MP: 97% ACN/3% NH_4Ac buffer at the pH of 6.0 for the two ZrO_2 -based columns; 85% ACN/15% NH_4Ac buffer at the pH of 6.0 for the SiO_2 column. Column temperature: 25 °C.

and pH of the MP [30–32]. An increasing number of reports [18–20,25,27–29,31,33–37] on thermodynamics in HILIC were found in recent years, which provided necessary theory guidance when column temperature was used as a variant regulating selectivity and analysis speed.

In RPLC and NPLC mode for high temperature separations, metallic oxides such as TiO_2 or ZrO_2 -based columns were used, which were reported to be stable up to 200 °C [1–3]. High column temperature offered lower back column pressure [31], shorter analysis time and higher column efficiency [33,37]. Given the

Table 3

The Zeta potential (ζ) of the three packings under different NH_4Ac concentrations.

Column	ζ (mV) Under different NH_4Ac concentrations				
	5 mM	50 mM	70 mM	90 mM	110 mM
MgO-ZrO_2	-30.73	-44.74	-58.59	-72.74	-79.52
ZrO_2	-24.56	-39.70	-72.47	-70.06	-80.20
SiO_2	-50.31	-54.87	-70.68	-78.29	-87.42

The ZrO_2 -based and SiO_2 packings were tested in 97% ACN with 3% NH_4Ac buffer and 85% ACN with 15% NH_4Ac buffer, respectively, at the pH of 6.0.

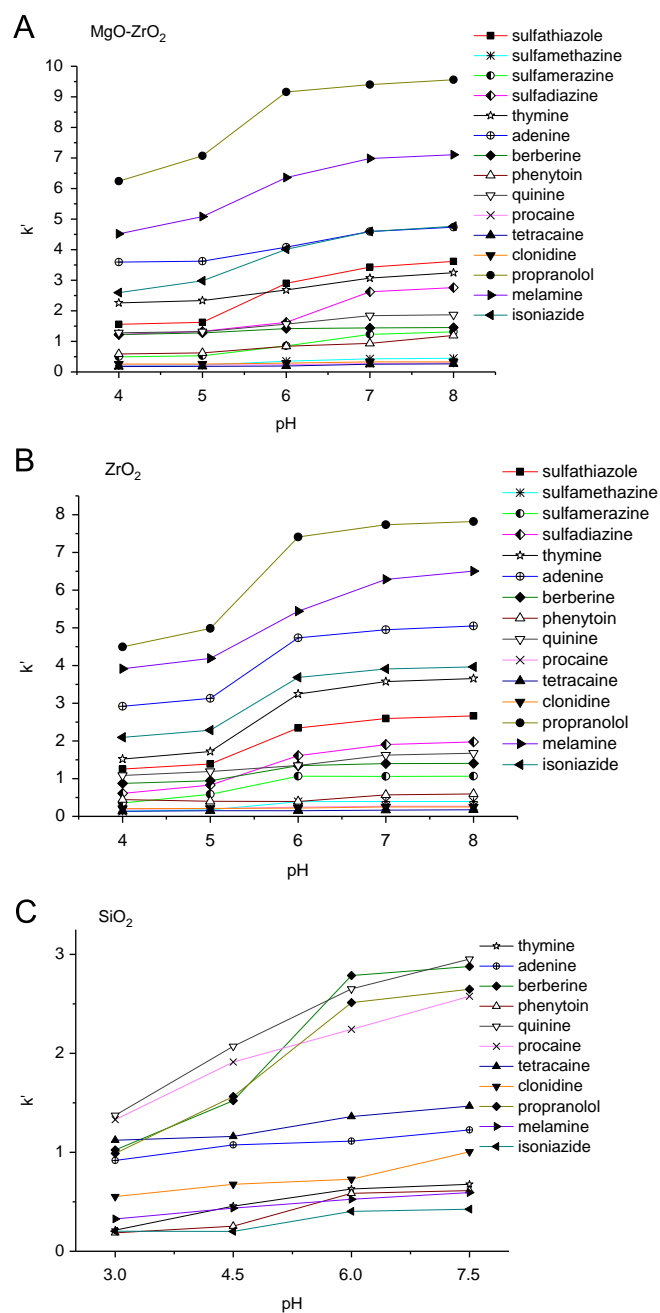


Fig. 5. Influence of MP pH on k' of the test solutes. (A) MgO-ZrO_2 ; (B) ZrO_2 ; (C) SiO_2 . MP: 97% ACN/3% aqueous buffer with 50 mM NH_4Ac for the two ZrO_2 -based columns; 85% ACN/15% aqueous buffer with 10 mM NH_4Ac for the SiO_2 column. Column temperature: 25 °C.

thermostability of MgO–ZrO₂ and ZrO₂ columns, it was of great significance to investigate the temperature influence on retention of the target solutes and explore the retention mechanism further on. In the present experiment, the retention behavior of the model compounds was studied under different column temperatures from 15 to 55 °C for the three columns. A commonly-used method to depict the chromatographic retention factor with column temperature is Van't Hoff equation:

$$\ln k' = -\frac{\Delta H^\theta}{RT} + \frac{\Delta S^\theta}{R} + \ln \Phi \quad (3)$$

where k' is the chromatographic retention factor of the analyte, ΔH^θ and ΔS^θ are the standard enthalpy and entropy transfer of a solute from the MP to SP, R is the molar gas constant and Φ is the volume phase ratio of the column which is constant for a given column and the corresponding MP. As seen from this equation, the plot of $\ln k'$ versus $1/T$ should be linear if ΔH^θ and ΔS^θ remain constant over the examined temperature range; contrarily, a non-linear plot could suggest changes of these parameters. Therefore,

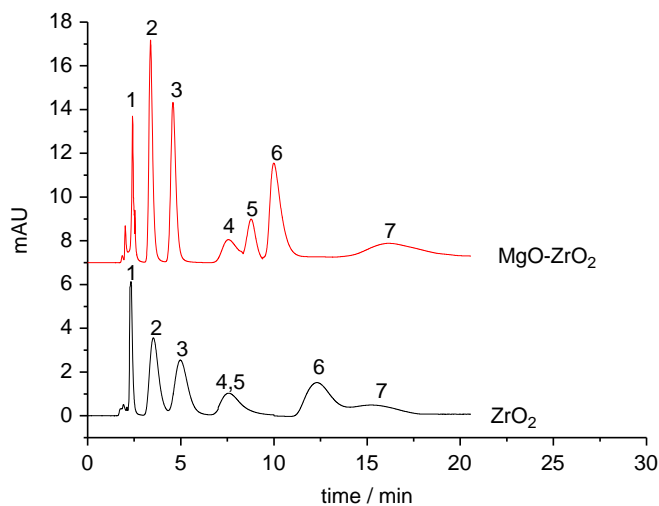


Fig. 6. The chromatograms of separation of seven basic compounds on the two ZrO₂-based columns. MP: 97% ACN/3% aqueous buffer with 50 mM NH₄Ac at the pH of 6.0. Column temperature: 55 °C. Wavelength: 275 nm. Peak identification: 1. sulfamethazine; 2. sulfamerazine; 3. sulfadiazine; 4. thymine; 5. sulfathiazole; 6. melamine; 7. propranolol.

Table 4

Parameters of Van't Hoff equation on the three columns.

Analytes	MgO–ZrO ₂				ZrO ₂				SiO ₂			
	ΔH^θ	ΔS^θ	ΔG^θ	r^2	ΔH^θ	ΔS^θ	ΔG^θ	r^2	ΔH^θ	ΔS^θ	ΔG^θ	r^2
Berberine	8.19	36.56	–2.72	0.9899	5.79	29.24	–2.94	0.9843	20.69	73.89	–1.34	0.9881
Propranolol	2.35	75.43	–20.17	0.9601	14.07	67.80	–6.17	0.9990	–4.16	–10.64	–1.01	0.9762
Thymine	5.49	32.73	–4.28	0.9620	7.39	41.07	–4.87	0.9836	–3.85	–11.75	–0.35	0.9025
Adenine	2.25	27.32	–5.91	0.9484	2.95	29.55	–5.87	0.9589	–10.41	–15.46	–5.87	0.9638
Melamine	–3.92	7.25	–6.08	0.9318	–1.66	18.09	–7.06	0.9995	16.21	68.01	–4.07	0.9915
Procaine	–9.84	–38.66	1.70	0.9146	–1.57	–9.48	1.26	0.9635	–25.68	–33.45	–15.71	0.9538
Tetracaine	–6.89	–30.88	2.33	0.9382	–2.26	–6.35	–0.36	0.9756	–7.26	–14.62	–2.90	0.9968
Clonidine	7.09	19.17	1.37	0.9858	9.56	31.85	0.05	0.9886	9.68	73.25	–12.16	0.9726
Quinine	13.25	65.89	–6.42	0.9825	18.76	79.46	–4.96	0.9735	–9.85	13.25	–13.8	0.9914
Isoniazide	23.74	92.16	–3.77	0.9788	20.18	81.68	–4.20	0.9924	–6.34	75.04	–10.60	0.9845
Phenytoin	6.03	24.59	–1.31	0.9613	10.36	48.37	–4.08	0.9690	–10.56	18.84	–16.18	0.9325
Sulfathiazole	9.57	47.10	–4.49	0.9849	50.58	186.69	–5.15	0.9854	–	–	–	–
Sulfamethazine	9.24	24.72	1.86	0.9701	13.62	44.09	0.46	0.9647	–	–	–	–
Sulfamerazine	4.28	18.29	–1.18	0.9391	2.96	20.56	–3.18	0.9332	–	–	–	–
Sulfadiazine	2.35	17.43	–2.85	0.8883	38.98	143.62	–3.89	0.9552	–	–	–	–

ΔH^θ (kJ/mol) and ΔS^θ (J/mol K) were calculated from the slope and intercept of Van't Hoff equation, respectively. ΔG^θ (kJ/mol) = $\Delta H^\theta - T\Delta S^\theta$. The volume phase ratio $\varphi = (V_w - V_M)/V_M$, $V_M = t_0 \times \nu$, where V_w was the geometric internal volume of the column, V_M and t_0 were the dead volume and dead time, respectively, and ν was the flow rate. The extra-column volume was neglected.

this plotting is usually used in the assessment of enthalpy and entropy changes for the exploration of retention mechanism [38].

The parameters, i.e. ΔH^θ , ΔS^θ and r^2 listed in Table 4, were calculated from the regression results of Van't Hoff equation. ΔG^θ was the Gibbs free energy. The r^2 of different analytes when plotting $\ln k'$ versus $1/T$ could indicate the change of retention mechanism. As seen from the result, the majority of the analytes showed good linearity on the three columns, which indicated that

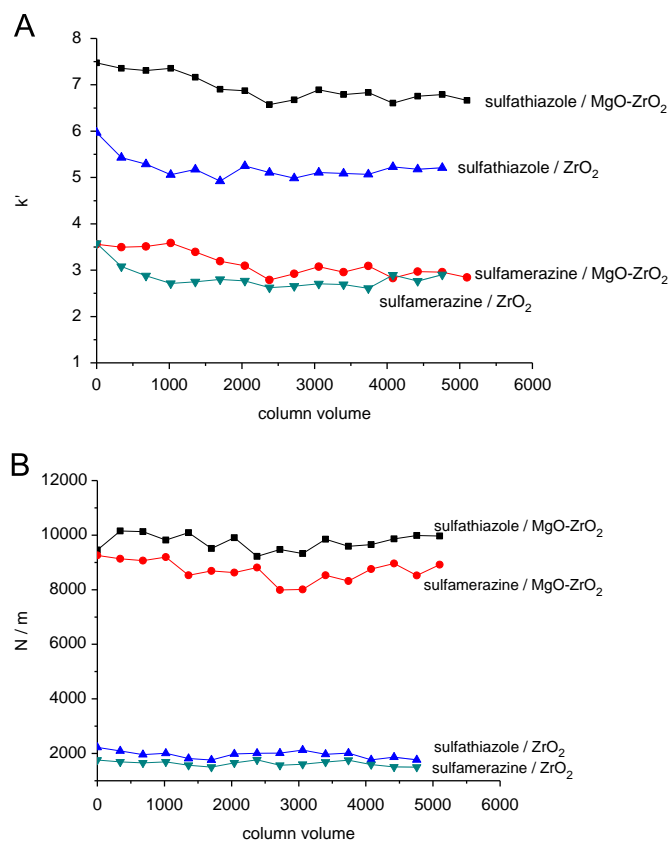


Fig. 7. Stability comparison for the two ZrO₂-based columns in terms of (A) k' and (B) column efficiency. MP: 97% ACN/3% aqueous buffer with 50 mM NH₄Ac at the pH of 6.0. Column temperature: 25 °C. Wavelength: 275 nm.

the retention mechanism remained the same despite of the varied column temperature.

Some publications [20,25,29,33–35] revealed that negative ΔH^θ indicated a single partitioning retention mechanism and an exothermic process of the analytes transferring from the MP to SP, while positive ΔH^θ indicated adsorptive mechanism and an endothermic process. As shown in Table 4, positive ΔH^θ values were obtained for almost all the analytes on MgO–ZrO₂ and ZrO₂ columns, implying an endothermic process based on adsorption interaction; thus high column temperature would facilitate the retention [20,37,39–41]. On the contrary, negative ΔH^θ values were obtained on the SiO₂ column, which suggested a spontaneous and exothermic process based on partitioning mechanism; thus high temperature would weaken the retention. For the two ZrO₂-based columns, the retention mechanism discussed herein was consistent with that obtained in Section 3.3.1. However, the negative ΔH^θ values for the SiO₂ column revealed a single partitioning mechanism, while the combination of adsorption and partitioning interaction was involved as the main mechanism in Section 3.3.1. This might be because column temperature primarily affected the thickness of the thin water layer immobilized on the SP surface within the studied temperature range [11,36], making partitioning interaction the main retention mechanism on the bare SiO₂ column. The contribution of this interaction to the overall retention was more significant than that of the adsorption interaction. As discussed by Bicker et al. [34], the retention of the analytes was hardly just dependent on HILIC-type partitioning for SiO₂-based packings. Actually, it was a multi/mixed-mode process in which HILIC-type weak adsorption and strong electrostatic interaction were also included.

From Eq. (3), the first term expressed the enthalpic retention contribution and the second term was the entropic change contribution. Therefore, both ΔH^θ and ΔS^θ participated jointly in the retention. For the two ZrO₂-based columns, the ΔH^θ of the majority analytes were positive and contributed negatively to the retention. Nevertheless, the positive and larger numerical ΔS^θ values (compared with ΔH^θ) could in some degree compensate the decrease of the retention, resulting in the negative ΔG^θ , which probably showed a classical entropy-driven (or entropically favorable) mechanism [25,36,42–44]. However, on the SiO₂ column, negative ΔH^θ values were obtained in most cases and contributed positively to the retention, but larger numerical and negative ΔS^θ values would weaken the retention, leading to the negative ΔG^θ , which probably indicated a classical enthalpy-driven (or enthalpically favorable) mechanism [36,42–46].

3.4. Comparison of the two ZrO₂-based columns

After optimization of various influencing variables (water content in MP, pH of the MP, concentration of NH₄Ac and column temperature), seven basic probe analytes were separated on the two ZrO₂-based columns as shown in Fig. 6. Under the same separation condition, MgO–ZrO₂ column exhibited superior chromatographic performance to the native ZrO₂ one, i.e. the analytes' responses and the number of theoretical plates were higher and the resolution between thymine and sulfathiazole was better. It could be explained that the addition of MgO into the native ZrO₂ would improve the surface chemical properties as well as the pore structure of the microparticles.

3.5. Stability test

The two ZrO₂-based columns were subjected to the stability test procedure elaborated in Section 2.5, with periodic evaluation of the two indicators, i.e. k' and the theoretical plates. As shown in Fig. 7, the overall tendency of the retention of the two solutes

decreased gradually, while the column efficiency almost stayed unchanged. In the case of MgO–ZrO₂ column, k' of the test solutes remained stable in the initial period (within 1000 column volumes), then it decreased to different degrees and finally kept fluctuating in a small range with the relative standard deviations (RSDs) of 4.3% and 8.9% for sulfathiazole and sulfadiazine, respectively. As for the bare ZrO₂ column, the RSDs of k' were in an acceptable range in spite of some fluctuations on the curves, 5.7% and 8.6% for sulfathiazole and sulfadiazine, respectively. The stability test revealed that the two SPs showed comparable stability and could remain stable within at least 5000 column volumes. In addition, it was worth of mention that the column efficiency on MgO–ZrO₂ column was almost five fold higher than that of the bare ZrO₂ column, as depicted in Fig. 7(B).

4. Conclusion

In this study, the bare ZrO₂ and MgO–ZrO₂ microparticles were employed as the hydrophilic interaction chromatographic (HILIC) stationary phases (SPs). Chromatographic performance of the two ZrO₂-based columns and a native SiO₂ column (for comparison) was systematically evaluated and some conclusions could be obtained as follows. (i) The retention of the analytes on the ZrO₂-based columns exhibited a “U-shape” mode which demonstrated that, in water-rich range, reversed phase liquid chromatography was the main mode; while, in ACN-rich range, HILIC was the main one. (ii) For HILIC mechanism, the increase of buffer concentration resulted in the decreased retention of the test solutes. (iii) The process of the analytes transferring from the MP to the ZrO₂-based SPs was endothermic and high column temperature would facilitate the retention. Contrarily, it was exothermic on the SiO₂ column. The main mechanism on the two ZrO₂-based columns was based predominantly on adsorptive interaction. Nevertheless, both adsorption and partitioning interaction contributed to retaining the analytes on the SiO₂ column. (iv) As for the MgO–ZrO₂ and ZrO₂ columns, the former was superior with its improved column efficiency and resolution, which signified that the addition of MgO into the ZrO₂ would improve the chromatographic behavior under HILIC mode. However, further investigations are still needed to elaborate significant information with respect to the multimodal retention mechanism of ZrO₂-based SPs in HILIC mode.

Acknowledgements

The authors gratefully acknowledge the financial support of this research by the Nature Science Foundation of China (No. 21075091 and No. 21105033), Program for New Century Excellent Talents in University (No. NCET-12-0213), Ministry of Education of China.

References

- [1] L. Janeckova, K. Kalikova, Z. Bosakova, E. Tesarova, J. Sep. Sci. 33 (2010) 3043–3051.
- [2] J. Nawrocki, C. Dunlap, A. McCormick, P.W. Carr, J. Chromatogr. A 1028 (2004) 1–30.
- [3] P. Jandera, K. Novotna, M.S. Beldean-Galea, K. Jisa, J. Sep. Sci. 29 (2006) 856–871.
- [4] J. Randon, S. Huguette, C. Demesmay, A. Berthod, J. Chromatogr. A 1217 (2010) 1496–1500.
- [5] J. Randon, S. Huguette, A. Piram, G. Puy, C. Demesmay, J.L. Rocca, J. Chromatogr. A 1109 (2006) 19–25.
- [6] J.A. Blackwell, P.W. Carr, J. Chromatogr. A 549 (1991) 43–57.
- [7] W.A. Schafer, P.W. Carr, J. Chromatogr. A 587 (1991) 149–160.
- [8] Q.H. Zhang, Y.Q. Feng, S.L. Da, Chromatographia 50 (1999) 654–657.

- [9] P.D.L. Mercera, J.G. Van Ommen, E.B.M. Doesburg, A.J. Burggraaf, J.R.H. Ross, *Appl. Catal.* 57 (1990) 127–148.
- [10] R. Thakkar, U. Chudasama, *Electrochim. Acta* 54 (2009) 2720–2726.
- [11] Q.H. Zhang, Y.Q. Feng, S.L. Da, *Anal. Sci.* 15 (1999) 767–772.
- [12] Y.L. Hu, Y.Q. Feng, J.D. Wan, S.L. Da, L. Hu, *Talanta* 54 (2001) 79–88.
- [13] Y.L. Hu, Y.Q. Feng, S.L. Da, *J. Liq. Chromatogr. Related Technol.* 24 (2001) 957–971.
- [14] Q.W. Yu, J. Yang, B. Lin, Y.Q. Feng, *Anal. Chim. Acta* 559 (2006) 79–88.
- [15] A. Alpert, *J. Chromatogr. A* 499 (1990) 177–196.
- [16] B. Dejaegher, D. Mangelings, Y.V. Heyden, *J. Sep. Sci.* 31 (2008) 1438–1448.
- [17] P. Hemstrom, K. Irgum, *J. Sep. Sci.* 29 (2006) 1784–1821.
- [18] A. Kumar, J.C. Heaton, D.V. McCalley, *J. Chromatogr. A* 1276 (2013) 33–46.
- [19] J. Wu, W. Bicker, W. Lindner, *J. Sep. Sci.* 31 (2008) 1492–1503.
- [20] R. Kucera, P. Kovarikova, M. Klivicky, J. Klimes, *J. Chromatogr. A* 1218 (2011) 6981–6986.
- [21] P. Kalafut, R. Kucera, J. Klimes, *J. Chromatogr. A* 1232 (2012) 242–247.
- [22] P. Kozlik, V. Simova, K. Kalikova, Z. Bosakova, D.W. Armstrong, E. Tesarova, *J. Chromatogr. A* 1257 (2012) 58–65.
- [23] M.A. Jaoude, J. Randon, *J. Chromatogr. A* 1218 (2011) 721–725.
- [24] G. Greco, S. Grosse, T. Letzel, *J. Chromatogr. A* 1235 (2012) 60–67.
- [25] L. Qiao, A. Dou, X. Shi, H. Li, Y. Shan, X. Lu, G. Xu, *J. Chromatogr. A* 1286 (2013) 137–145.
- [26] Z. Yang, *J. Biotechnol.* 144 (2009) 12–22.
- [27] H. Qiu, L. Loukotkova, P. Sun, E. Tesarova, Z. Bosakova, D.W. Armstrong, *J. Chromatogr. A* 1218 (2011) 270–279.
- [28] Y. Guo, S. Srinivasan, S. Gaiki, *Chromatographia* 66 (2007) 223–229.
- [29] A. Shen, Z. Guo, X. Cai, X. Xue, X. Liang, *J. Chromatogr. A* 1228 (2012) 175–182.
- [30] H.A. Claessens, M.A. van Straten, *J. Chromatogr. A* 1060 (2004) 23–41.
- [31] G. Paglia, O. D'Apolito, F. Tricarico, D. Garofalo, G. Corso, *J. Sep. Sci.* 31 (2008) 2424–2429.
- [32] L. Dong, J. Huang, *Chromatographia* 65 (2007) 519–526.
- [33] Z. Hao, B. Xiao, N. Weng, *J. Sep. Sci.* 31 (2008) 1449–1464.
- [34] W. Bicker, J. Wu, H. Yeman, K. Albert, W. Lindner, *J. Chromatogr. A* 1218 (2011) 882–895.
- [35] W. Bicker, J. Wu, M. Laemmerhofer, W. Lindner, *J. Sep. Sci.* 31 (2008) 2971–2987.
- [36] H. Qiu, D.W. Armstrong, A. Berthod, *J. Chromatogr. A* 1272 (2013) 81–89.
- [37] Z. Hao, C.-Y. Lu, B. Xiao, N. Weng, B. Parker, M. Knapp, C.-T. Ho, *J. Chromatogr. A* 1147 (2007) 165–171.
- [38] S.D. Allmon, J.G. Dorsey, *J. Chromatogr. A* 1216 (2009) 5106–5111.
- [39] Y. Guo, S. Gaiki, *J. Chromatogr. A* 1074 (2005) 71–80.
- [40] C.B. Castells, L.G. Gagliardi, C. Rafols, M. Roses, E. Bosch, *J. Chromatogr. A* 1042 (2004) 23–35.
- [41] M.J. Christopherson, K.J. Yoder, J.T. Hill, *J. Liq. Chromatogr. Related Technol.* 29 (2006) 2545–2558.
- [42] C.S. Lee, W.J. Cheong, *J. Chromatogr. A* 848 (1999) 9–20.
- [43] D. Cho, S. Park, J. Hong, T. Chang, *J. Chromatogr. A* 986 (2003) 191–198.
- [44] G.E. Rowe, H. Aomari, T. Chevaldina, M. Lafrance, S. St-Arnaud, *J. Chromatogr. A* 1177 (2008) 243–253.
- [45] A. Peter, E. Veves, D.W. Armstrong, *J. Chromatogr. A* 958 (2002) 89–107.
- [46] A. Peter, G. Torok, D.W. Armstrong, G. Toth, D. Tourwe, *J. Chromatogr. A* 828 (1998) 177–190.